

**UC Berkeley**  
**SEMM Reports Series**

**Title**

Transient Wave Propagation in Transversely Isotropic Rods

**Permalink**

<https://escholarship.org/uc/item/5mj3b05s>

**Authors**

Mengi, Yalcin

McNiven, Hugh

**Publication Date**

1969-12-01

R

Report No. 69-23

STRUCTURES AND MATERIALS RESEARCH  
DEPARTMENT OF CIVIL ENGINEERING

---

---

# TRANSIENT WAVE PROPAGATION IN TRANSVERSELY ISOTROPIC RODS

by  
Y. MENGI  
and  
H. D. McNIVEN

Report to  
National Science Foundation  
NSF Grant GK-10070

---

---

December 1969

STRUCTURAL ENGINEERING LABORATORY  
UNIVERSITY OF CALIFORNIA  
BERKELEY CALIFORNIA

Structures and Materials Research  
Department of Civil Engineering  
Division of Structural Engineering

Report No. 69-23

TRANSIENT WAVE PROPAGATION IN  
TRANSVERSELY ISOTROPIC RODS

by

Y. Mengi

Research Assistant  
University of California  
Berkeley, California, 94720

and

H. D. McNiven

Professor of Engineering Science  
University of California  
Berkeley, California, 94720

Structural Engineering Laboratory  
University of California  
Berkeley, California, 94720

December 1969

## I. Introduction

This is a study of the response in a transversely isotropic rod to a transient input on its end. The material of the rod is arranged so that the axis of the rod is parallel to axes of isotropy. The input on the end is not entirely arbitrary in that we specify that it will be a uniform normal pressure, but its time dependency is left open to choice. The rod is circular and, as we do not consider a boundary at its far end, is taken as semi-infinite.

In finding such a response in a rod, one must choose, in the beginning whether he seeks the response at stations near the input end or far from the end. The choice is important in deciding the mathematical method that is to be used. The choice here is to find the responses at stations near the end of the rod. This choice does not dictate the method but it narrows the possibilities.

Three methods have been used successfully for the comparable problem for isotropic rods. One method was used by Miklowitz<sup>[1]</sup> who employed integral transform method, then with the use of numerical integration he obtained the response near the end of the rod. His study is based on an approximate theory due to Mindlin and Herrmann<sup>[2]</sup> The second is due to Bertholf<sup>[3]</sup> who used the exact three dimensional theory of elasticity and solved the equations using finite differences. The third solution technique is the method of characteristics. It is the method of characteristics that is used here.

The method of characteristics, though not unworkable when applied to differential equations having more than two independent variables, is appropriate for solving equations with two independent variables usually

one space variable and time. With these two variables one is able to work conveniently on the space-time plane. Before using the method of characteristics one must have at hand an approximate theory, employing the two independent variables suggested, which describes accurately the motions in transversely isotropic, circular rods. At the beginning of the study no such theory was available, so the theory had to be developed. This theory is presented in a paper by Mengi and McNiven.<sup>[4]</sup> It is a three-mode theory resembling closely a theory for isotropic rods by Mindlin and McNiven<sup>[5]</sup> and was developed examining closely the behavior of motions in a transversely isotropic rod dictated by the frequency equation derived from the field equations of three dimensional elasticity. This exact frequency equation was derived by McNiven and Mengi.<sup>[6]</sup> As the matching of the spectral lines from the approximate theory and the lowest three modes of the exact theory was excellent, we feel confident that by using the approximate theory we can predict accurately the response in a rod except perhaps for the very front of the wave which would be influenced by the higher branches omitted in the theory.

Using method of characteristics we exploit two circumstances. First, the approximate equations are hyperbolic, a necessary condition for real wave propagation velocities, and second because the lines on the space-time plane, which represent wave fronts, coincide with characteristic lines along which the governing equations take a greatly simplified, degenerate form.

Using the method of characteristics one is able to reduce the governing equations of the three-mode theory to two types of equations. The first type is decay equations which are integrated directly on the space-time plane to find the behavior on the first wave front. We explore the domain behind the first wave front by means of the conical form of the

governing equations. These are valid along characteristic lines and are integrated using finite differences.

We assume knowledge of the method of characteristics so we do not review the method here. What explanation there is, is contained in the section on numerical analysis because the numerical method we use is not always used when employing characteristics.

In the general theory the elastic constants are left undefined and the time dependency of the input is left arbitrary. In the numerical analysis both are specified. We take as our input a step function in time and find the responses in rods of two different materials. The first is a fiber reinforced rod and the second is magnesium. The responses are found at a station approximately one diameter from the end of the rod. For each of the two materials we calculate four responses. We find the radial strain  $\epsilon_{rr}$ , the axial strain  $\epsilon_{zz}$  both on the lateral surface and along the axis of the rod, and finally the generalized axial stress  $P_z$ . The responses in the fiber reinforced rod are seen in Figures 2, 3 and 4 and in the magnesium rod in Figures 5, 6 and 7.

The results are not easy to appraise as there appears to be no other study of transversely isotropic rods with which the results could be compared. However, from our studies, and those of others, on isotropic rods it is possible to state that of all of the results the only obvious inaccuracy is contained in the axial strain on the lateral surface for both materials. The front of the wave will not be stepped as our results show, but will start at the origin and rise with a fairly steep slope.

## II. The Approximate Theory

The approximate theory governing the axisymmetric motions in transversely isotropic rods was derived in a previous paper<sup>[4]</sup> and will be described in the barest outline here.

The rod is circular and has a radius "a". It is referred to a cylindrical coordinate system  $(r, \theta, z)$  within which the center of the end of the rod is located at the origin and positive  $z$  is measured along the axis of the rod. The material is arranged so that axes of isotropy are parallel to the axis of the rod. The transversely isotropic material is identified by five elastic constants  $c_{11}$ ,  $c_{12}$ ,  $c_{13}$ ,  $c_{33}$  and  $c_{44}$ .

In the development which follows, when it is appropriate, we use indicial notation and all the rules that apply to its use.

The theory is derived from the constitutive equation

$$\tau_{\alpha} = c_{\alpha\beta} \epsilon_{\beta} \quad (\alpha, \beta = 1, \dots, 6) \quad , \quad (1)$$

where

$$(\tau_{\alpha}) = (\tau_{rr}, \tau_{\theta\theta}, \tau_{zz}, \tau_{\theta z}, \tau_{zr}, \tau_{r\theta})$$

$$(\epsilon_{\alpha}) = (\epsilon_{rr}, \epsilon_{\theta\theta}, \epsilon_{zz}, 2\epsilon_{\theta z}, 2\epsilon_{zr}, 2\epsilon_{r\theta})$$

and

$$(c_{\alpha\beta}) = \begin{bmatrix} c_{11} & c_{12} & c_{13} & 0 & 0 & 0 \\ c_{12} & c_{11} & c_{13} & 0 & 0 & 0 \\ c_{13} & c_{13} & c_{33} & 0 & 0 & 0 \\ 0 & 0 & 0 & c_{44} & 0 & 0 \\ 0 & 0 & 0 & 0 & c_{44} & 0 \\ 0 & 0 & 0 & 0 & 0 & \frac{1}{2}(c_{11}-c_{12}) \end{bmatrix} \quad , \quad (2)$$

$\tau_{ij}$ ,  $\epsilon_{ij}$  being stress and strain tensors respectively.

The theory is described in terms of generalized displacements  $u$ ,  $w$  and  $\psi$  which are related to the radial and axial displacements  $u_r$  and  $u_z$  according to

$$\begin{aligned} u_r &= \bar{r}u(x, \tau) \\ u_z &= w(x, \tau) + (1 - 2\bar{r}^2)\psi(x, \tau) \end{aligned} \quad (3)$$

where  $\bar{r} = r/a$ ;  $r$  is the radial distance.

The constitutive equations relating these generalized displacements and generalized forces are

$$\begin{aligned} \left(\frac{a}{c_{444}}\right) P_r &= K_1^2(2 - \gamma_k) \frac{\gamma_q}{\gamma_s} u + \delta K_1(\gamma_q - 1)w_{,x} \\ 2 \left(\frac{a}{c_{444}}\right) P_z &= \delta \gamma_n^2 w_{,x} + 2K_1(\gamma_q - 1)u \\ 4 \left(\frac{a}{c_{444}}\right) P_{rz} &= K_2^2(\delta u_{,x} - 4\psi) \\ 6 \left(\frac{a}{c_{444}}\right) P_\psi &= \delta \gamma_n^2 \psi_{,x} \end{aligned} \quad (4)$$

where the generalized forces are defined by

$$\begin{aligned} P_r &= \int_0^1 (\tau_{rr} + \tau_{\theta\theta}) \bar{r} d\bar{r} \\ P_z &= \int_0^1 \tau_{zz} \bar{r} d\bar{r} \\ P_{rz} &= \int_0^1 \tau_{rz} \bar{r}^2 d\bar{r} \\ P_\psi &= \int_0^1 \tau_{zz} (1 - 2\bar{r}^2) \bar{r} d\bar{r} \end{aligned} \quad (5)$$



The strains are given in terms of the generalized displacements according to

$$\begin{aligned}\epsilon_{rr} &= K_1 \frac{u}{a} \\ \epsilon_{\theta\theta} &= K_1 \frac{u}{a} \\ \epsilon_{zz} &= \frac{\delta}{a} \left\{ w_{,x} + (1 - 2\bar{r}^2)\psi_{,x} \right\} \\ \epsilon_{rz} &= K_2 \frac{\bar{r}}{2a} (\delta u_{,x} - 4\psi) \\ \epsilon_{\theta z} &= \epsilon_{r\theta} \equiv 0 .\end{aligned}\tag{6}$$

The theory is contained in the three equations

$$\begin{aligned}\delta K_2^2 (\delta u_{,xx} - 4\psi_{,x}) - 4K_1^2 (2 - \gamma_k) \frac{\gamma_q}{\gamma_s} u - 4K_1 (\gamma_q - 1) \delta w_{,x} + \frac{4a}{c_{44}} R &= K_3^2 \delta^2 u_{,\tau\tau} \\ \delta \gamma_n^2 w_{,xx} + 2K_1 (\gamma_q - 1) u_{,x} + \frac{2a}{\delta c_{44}} Z &= \delta w_{,\tau\tau} \\ \delta^2 \gamma_n^2 \psi_{,xx} + 6K_2^2 (\delta u_{,x} - 4\psi) - \frac{6a}{c_{44}} Z &= \delta^2 K_4^2 \psi_{,\tau\tau} .\end{aligned}\tag{7}$$

In Eqs.(3-7);  $R = \tau_{rr} \Big|_{r=a}$ ,  $Z = \tau_{rz} \Big|_{r=a}$ , and

$$\begin{aligned}x &= \frac{\delta z}{a} , && \text{a dimensionless distance} \\ \tau &= \frac{\delta t}{a} \left( \frac{c_{44}}{\rho} \right)^{1/2} , && \text{a dimensionless time}\end{aligned}\tag{8}$$

and

$$\begin{aligned}\gamma_q &= \frac{c_{13} + c_{44}}{c_{44}} ; && \gamma_s = \frac{c_{13} + c_{44}}{c_{11}} ; \\ \gamma_n &= \left( \frac{c_{33}}{c_{44}} \right)^{1/2} ; && \gamma_k = \frac{c_{11} - c_{12}}{c_{11}} ;\end{aligned}\tag{9}$$

$\rho$  is the mass density.

$\delta$  is a constant defined as the first nonzero root of  $J_1(\delta_m) = 0$  [6],  $J_1$  being the Bessel function of the first kind.

The  $K_i$ 's ( $i = 1 - 4$ ) are adjustment factors introduced in the theory to make the three spectral lines of the theory match more closely the lowest three branches of the exact theory. They are functions of the material constants  $c_{\alpha\beta}$ .

### III. Formulation of the Problem

The formulation begins by putting the governing equations, Eqs. (7), in the form

$$u_i'_{,xx} - \frac{1}{c_i} u_i'_{,tt} = \alpha_{ij} u_j + \beta_{ij} u_j'_{,x} \quad (i, j = 1, \dots, n) \quad (10)$$

(no sum on  $i$ )

This is achieved if we let

$$(\alpha_{ij}) = \begin{bmatrix} 0 & 0 & 0 \\ 0 & \frac{24K_2^2}{\delta^2 \gamma_n^2} & 0 \\ 0 & 0 & \frac{4K_1^2(2 - \gamma_k)\gamma_g}{\delta^2 K_2^2 \gamma_s} \end{bmatrix}$$

(11)

$$(\beta_{ij}) = \begin{bmatrix} 0 & 0 & -\frac{2K_1(\gamma_g - 1)}{\delta \gamma_n^2} \\ 0 & 0 & -\frac{6K_2^2}{\delta \gamma_n^2} \\ \frac{4K_1(\gamma_g - 1)}{\delta K_2^2} & \frac{4}{\delta} & 0 \end{bmatrix},$$

and if we take

$$(u_1, u_2, u_3) = (w, \psi, u) \text{ and}$$

$$c_1^2 = \gamma_n^2; \quad c_2^2 = \frac{\gamma_n^2}{K_4^2}; \quad c_3^2 = \frac{K_2^2}{K_3^2}.$$

Eqs. (10) constitute a system of linear hyperbolic equations for which the method of characteristics was discussed in detail in a paper by Mengi and McNiven. [7]

For a reasonable range of values of  $c_{\alpha\beta}$  we assume that

$$c_1^2 > c_2^2 > c_3^2. \quad (12)$$

We note that  $c_1 = \gamma_n$  is the dimensionless form of the longitudinal wave velocity  $\left(\frac{c_{33}}{\rho}\right)^{1/2}$ .

Even though the method of characteristics is general and could be used to handle a large variety of boundary and initial conditions, we are concerned here with a specific problem, namely the response of a semi-infinite rod, initially at rest, whose cylindrical surface is free of traction, and subjected to a uniform pressure on the end of the rod that has an arbitrary dependence on time. The boundary conditions take the form;

$$R = Z = 0$$

$$\tau_{zz}(0, \tau) = -f(\tau)H(\tau) \quad (13)$$

$$\tau_{rz}(0, \tau) = 0.$$

In Eqs. (13),  $H(\tau)$  is the usual Heaviside step function and  $f(\tau)$  is a prescribed, continuous function of time.

In terms of the generalized forces the boundary conditions on the end of the rod can be written:

$$\begin{aligned}
 P_z(0, \tau) &= \frac{-f(\tau)H(\tau)}{2} \\
 P_\psi(0, \tau) &= 0 \\
 P_{rz}(0, \tau) &= 0
 \end{aligned}
 \tag{14}$$

Using Eq. (4) these conditions can be expressed in terms of the generalized displacements according to

$$\begin{aligned}
 pw_x(0, \tau) + qu(0, \tau) &= g(\tau)H(\tau) \\
 \psi_x(0, \tau) &= 0 \\
 \delta u_x(0, \tau) - 4\psi(0, \tau) &= 0
 \end{aligned}
 \tag{15}$$

where

$$p = \frac{\delta \gamma_n^2}{2}; \quad q = K_1(\gamma_q - 1); \quad g(\tau) = -\frac{af(\tau)}{2c_{44}}.
 \tag{16}$$

The initial conditions are

$$\begin{aligned}
 u(x, 0) = u_\tau(x, 0) &= 0 \\
 w(x, 0) = w_\tau(x, 0) &= 0 \\
 \psi(x, 0) = \psi_\tau(x, 0) &= 0
 \end{aligned}
 \tag{17}$$

The problem is one of finding solutions of Eqs. (10) subject to the boundary and initial conditions given by Eqs. (15) and (17).

#### IV. The Method of Characteristics

The rod behavior we are seeking is the response to an input of normal stress on the end of the rod. As the resulting disturbances will

move down the rod, the behavior is best understood if it is described using the notion of wave fronts. The first wave front is defined as the boundary between disturbed and undisturbed regions of the rod, while second, third etc., wave fronts are related to the notion of the arrival of the additional disturbances to an already disturbed material point. When the material at a point becomes suddenly disturbed from an undisturbed state or when an already disturbed material point has some additional disturbance, it can only do so if some derivatives of the displacement vector suffers a finite jump at the point. On the  $x - \tau$  plane, a wave front can be represented by a line and by definition that line will be a characteristic. In our problem the initial conditions are all zero which means that of a family of characteristic lines, it is the ones emanating from the origin of the  $x - \tau$  plane that will be the wave fronts. The order of discontinuity of the characteristic lines describing the wave fronts will depend on the boundary conditions on the end of the rod, specifically the dependence on time in the neighborhood of  $\tau = 0$ .

Since Eqs. (10) represent three equations, there will be three wave fronts,  $S_1$ ,  $S_2$ , and  $S_3$ , shown in Fig. 1. In the boundary conditions Eqs. (13),  $f(\tau)$  is an arbitrary continuous function of  $\tau$ . If  $f(0) \neq 0$ , we will show shortly that along  $S_1$  the first derivatives of  $w$  will suffer a finite jump, higher order derivatives of  $u$  and  $\psi$  will have finite jumps and that along  $S_2$  and  $S_3$  the discontinuities will be of order two or higher for all three generalized displacements. As  $S_1$  is a characteristic line of first order discontinuity in  $w$ , it is necessary to use decay equations to find  $w_{,x}$  and  $w_{,\tau}$  along  $S_1$  immediately behind the wave front.

We turn to the decay equations themselves, Eqs. (20), (21) in reference (7), as they apply to  $S_1$ ,  $S_2$ , and  $S_3$ , and note from the second of Eqs. (11) that  $\beta_{11} = \beta_{22} = \beta_{33} = 0$ . The decay equations are therefore,

$$\begin{aligned} [w, x] &= A_1, & [w, \tau] &= -c_1 A_1 & \text{along } S_1 \\ [\psi, x] &= A_2, & [\psi, \tau] &= -c_2 A_2 & \text{along } S_2 \\ [u, x] &= A_3, & [u, \tau] &= -c_3 A_3 & \text{along } S_3. \end{aligned} \quad (18)$$

In Eqs. (18) a set of square brackets implies a finite jump of the function they enclose.

The  $A_i$ 's are constants obtained from the behavior of the boundary and initial conditions in the neighborhood of the origin of the  $(x - \tau)$  plane. Using boundary conditions Eqs. (15) and initial conditions Eqs. (17), and noting that  $[u] = [w] = [\psi] = 0$  everywhere in the  $(x - \tau)$  plane one obtains

$$\begin{aligned} [w, x(0, 0)] &= \frac{g(0)}{p} \\ [\psi, x(0, 0)] &= 0 \\ [u, x(0, 0)] &= 0. \end{aligned} \quad (19)$$

Comparing Eqs. (18) and (19) we can identify

$$\begin{aligned} A_1 &= \frac{g(0)}{p} \\ A_2 &= A_3 = 0. \end{aligned} \quad (20)$$

Accordingly the decay equations are

$$\begin{aligned}
[w,_{x}] &= \frac{g(0)}{p}, & [w,_{\tau}] &= -\frac{c_1 g(0)}{p} & \text{along } S_1 \\
[\psi,_{x}] &= 0, & [\psi,_{\tau}] &= 0 & \text{along } S_2 \\
[u,_{x}] &= 0, & [u,_{\tau}] &= 0 & \text{along } S_3.
\end{aligned} \tag{21}$$

It is worth noting that three mode approximate theory indicates no decay of the first derivatives of the generalized displacements.

From Eqs. (21) and from the fact that  $f(\tau)$  is a continuous function of  $\tau$  we conclude that in the disturbed region behind the wave front  $S_1$  all of the first derivatives of the generalized displacements are continuous so that the canonical form of the equations are appropriate. Within the framework of the approximate theory these equations, Eqs. (16) in reference (7), have the form,

$$\begin{aligned}
\mp d(w,_{x}) - \frac{1}{c_1} d(w,_{\tau}) &= \mp dx \beta_{13} u,_{x} & \text{along } \frac{dx}{d\tau} &= \mp c_1 \\
\mp d(\psi,_{x}) - \frac{1}{c_2} d(\psi,_{\tau}) &= \mp dx (\alpha_{22} \psi + \beta_{23} u,_{x}) & \text{along } \frac{dx}{d\tau} &= \mp c_2 \\
\mp d(u,_{x}) - \frac{1}{c_3} d(u,_{\tau}) &= \mp dx (\alpha_{33} u + \beta_{31} w,_{x} + \beta_{32} \psi,_{x}) & \text{along } \frac{dx}{d\tau} &= \mp c_3.
\end{aligned} \tag{22}$$

Along with the six equations of Eqs. (22) we exploit the fact that the displacement field is continuous and differentiable, so that along any line on the  $x - \tau$  plane

$$\begin{aligned}
dw &= w,_{x} dx + w,_{\tau} d\tau \\
d\psi &= \psi,_{x} dx + \psi,_{\tau} d\tau \\
du &= u,_{x} dx + u,_{\tau} d\tau
\end{aligned} \tag{23}$$

giving us nine working equations.

## V. Numerical Analysis

We seek the generalized displacements  $u$ ,  $\psi$  and  $w$  and their first derivatives at a station  $x$  and at a time  $\tau$ , and having these we can calculate the strains and stresses. We refer to Figure 1, which shows the  $(x - \tau)$  plane. On this plane, the line  $S_1(x - c_1\tau = 0)$  divides the space-time domain into two parts, the domain  $D_1$  representing undisturbed particles and  $D_2$  representing particles of the rod which are in motion. The part  $D_2$ , which is the part that interests us, is subdivided by means of one primary and two secondary grids. The primary grid, shown by fine solid lines, is formed by two sets of parallel lines. The first set ( $x - c_1\tau = \text{const}$ ) is parallel to the line  $S_1$ , and second set ( $x + c_1\tau = \text{const}$ ) has equal but opposite slopes. Each diamond shaped element has diagonals measuring  $2\Delta x$  and  $2\Delta\tau$ . The secondary sets of grid lines are members of the families  $x \pm c_2\tau = \text{constant}$  and  $x \pm c_3\tau = \text{constant}$ . They are shown dotted in Figure 1, and are used when analyzing an individual element. As the dotted lines fall within the element, the domain of dependence of a point is conserved.

In what follows the nine quantities  $u$ ,  $u_{,x}$ ,  $u_{,\tau}$ ,  $\psi$ ,  $\psi_{,x}$ ,  $\psi_{,\tau}$ ,  $w$ ,  $w_{,x}$ ,  $w_{,\tau}$  are considered, for convenience, to be the nine elements of the vector  $y_i$ . To establish  $y_i$  in the region  $D_2$ , we start at the origin and along  $S_1$ , where they are known from the decay equations, and fan out into the region element by element. To be more explicit, we know  $y_i$  at the points 0 and 1 in Figure 1, and using a technique to be explained shortly, we find  $y_i$  at the point 2. Having  $y_i$  at the points 1, 2, and 3, we use the same technique to find  $y_i$  at the point 4, and so forth.



In explaining the technique we refer to element M shown in Figure 1, and to its detached enlargement. The  $y_i$ 's are known at points  $A_1$ ,  $A_7$  and  $A_2$  and are sought at the point A. As there are nine unknowns, we need nine equations to establish them.

The boundary lines  $AA_1$  and  $AA_2$  are the characteristic lines  $x_1 - c_1\tau = \text{constant}$ , and  $x + c_1\tau = \text{constant}$  respectively. Through the point A we draw the characteristic lines  $AA_3$  and  $AA_4$  with slopes  $\pm c_2$ , and characteristic lines  $AA_5$  and  $AA_6$  with slopes  $\pm c_3$ . The values of  $y_i$  are calculated at  $A_3$  and  $A_5$  by interpolating the values at  $A_1$  and  $A_7$ , and at  $A_4$  and  $A_6$  by interpolating the values at  $A_7$  and  $A_2$ . Six of the nine equations come from using six canonical equations, Eqs. (22), one each along the six characteristic lines per element converging on A.

The three remaining equations are equations (23). As these are valid for any line in the  $(x - \tau)$  plane, we choose to use them along the diagonal line  $AA_7$  ( $x = \text{constant}$ ). The nine elements of  $y_i$  are found at A by solving the nine equations by the method of finite differences.

For an element L adjacent to the line  $x = 0$ , the procedure is the same except that the three equations along the three lines  $x - c_i\tau = \text{constant}$  ( $i = 1, 2, 3$ ) must be replaced by the end boundary conditions at  $x = 0$ , Eqs. (15);

$$pw_{,x}(A) + qu(A) = g(A)$$

$$\psi_{,x}(A) = 0 \quad (24)$$

$$\delta u_{,x}(A) - 4\psi(A) = 0 .$$

When one is dealing with numerical methods of this kind, convergence must be considered. In the Appendix of reference (7), it is shown

that for a fixed point  $(x^*, \tau^*)$  on the  $(x - \tau)$  plane, the error becomes zero as the mesh size  $\Delta\tau$  goes to zero.

## VI. Numerical Results

The choice is to calculate and exhibit three quantities: the radial strain  $\epsilon_{rr}$ , the axial force  $P_z$  and the axial strain  $\epsilon_{zz}$ . For an input on the end of the rod,  $f(\tau) = P_0$  (a constant) is chosen. With the method of characteristics  $f(\tau)$  can be an arbitrary function and this particular choice is made for the following reason; as the three mode approximate theory is limited to frequencies less than that of the cut-off frequency of the second axial shear mode, it is advisable to choose an input function for which the magnitude of its Fourier transform decreases with increasing frequency. The Fourier transform of  $P_0$  decreases as  $(1/\omega)$  with increasing frequency.

Numerical results are found for two different rods. One (rod 1) is made of a fiber reinforced material having the material constants

$$\frac{c_{11}}{c_{33}} = 0.472 ; \quad \frac{c_{12}}{c_{33}} = 0.165 ;$$

(25)

$$\frac{c_{13}}{c_{33}} = 0.176 ; \quad \frac{c_{44}}{c_{33}} = 0.104 ,$$

and the other (rod 2) is made of magnesium having the material constants

$$\frac{c_{11}}{c_{33}} = 0.954 ; \quad \frac{c_{12}}{c_{33}} = 0.390 ;$$

(26)

$$\frac{c_{13}}{c_{33}} = 0.326 ; \quad \frac{c_{44}}{c_{33}} = 0.277 .$$

Numerical analysis is carried out using a mesh size dictated by  $\Delta x = 0.10$ . The response is evaluated at the station  $x = 7.60$ , about one diameter from the end of the rod. The responses are shown in Figures (2-4) for material 1 and in Figures (5-7) for material 2. The approximate theory accommodates a distribution of the axial strain across a rod cross section and so Figures 3 and 6 show a plot of this strain at the center of the rod as well as on its lateral surface. The computations show that at any station,  $\epsilon_{rr}$ ,  $\epsilon_{zz}$  and  $P_z$  asymptotically approach their static values as time increases indefinitely, which ensures the stability of the numerical procedure.

#### Acknowledgment

This study was sponsored by a grant provided to the University of California by the National Science Foundation.

## REFERENCES

1. J. Miklowitz, J. Appl. Mech., 24, 231 (1957).
2. R. D. Mindlin and G. Herrmann, Proceedings of the First U.S. National Congress of Appl. Mech., 187 (1952).
3. L. D. Bertholf, Trans. Am. Soc. Mech. Engrs., J. Appl. Mech., 89, 725 (1967).
4. Y. Mengi and H. D. McNiven, to be published.
5. R. D. Mindlin and H. D. McNiven, J. Appl. Mech., 82E, 145 (1960).
6. H. D. McNiven and Y. Mengi, to be published.
7. Y. Mengi and H. D. McNiven, accepted for publication by the International Journal of Solids and Structures.

## REFERENCES

1. J. Miklowitz, J. Appl. Mech., 24, 231 (1957).
2. R. D. Mindlin and G. Herrmann, Proceedings of the First U.S. National Congress of Appl. Mech., 187 (1952).
3. L. D. Bertholf, Trans. Am. Soc. Mech. Engrs., J. Appl. Mech., 89, 725 (1967).
4. Y. Mengi and H. D. McNiven, to be published.
5. R. D. Mindlin and H. D. McNiven, J. Appl. Mech., 82E, 145 (1960).
6. H. D. McNiven and Y. Mengi, to be published.
7. Y. Mengi and H. D. McNiven, accepted for publication by the International Journal of Solids and Structures.

## CAPTIONS FOR FIGURES

Fig. 1 Description of characteristic lines and wave fronts on the  $(x - \tau)$  plane.

Fig. 2 Radial strain for rod 1 at the station  $z \approx 1$  diam.

Fig. 3 Axial strain for rod 1 at the station  $z \approx 1$  diam.

Fig. 4 Axial generalized force for rod 1 at the station  $z \approx 1$  diam.

Fig. 5 Radial strain for rod 2 at the station  $z \approx 1$  diam.

Fig. 6 Axial strain for rod 2 at the station  $z \approx 1$  diam.

Fig. 7 Axial generalized force for rod 2 at the station  $z \approx 1$  diam.

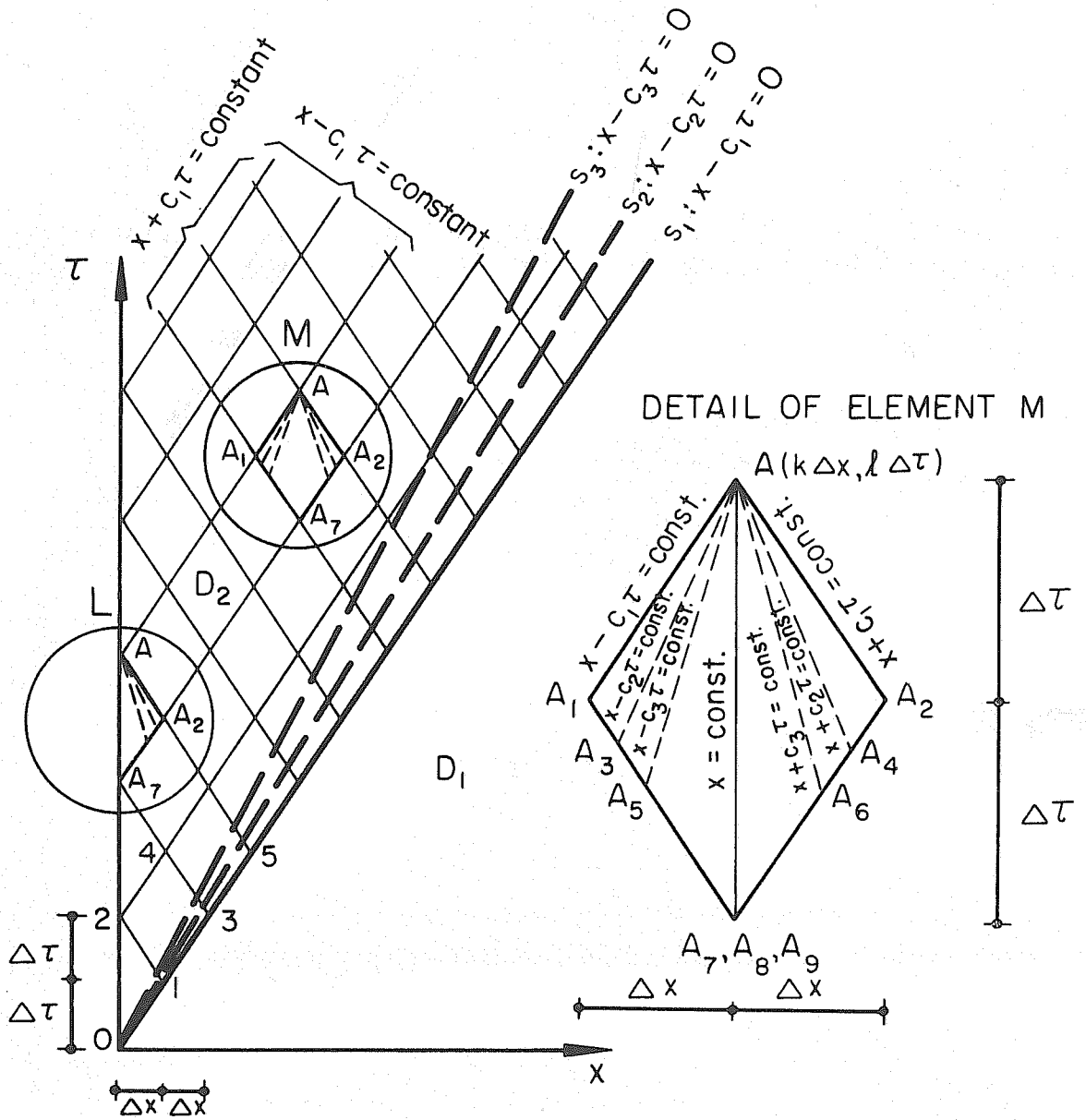


FIG. 1

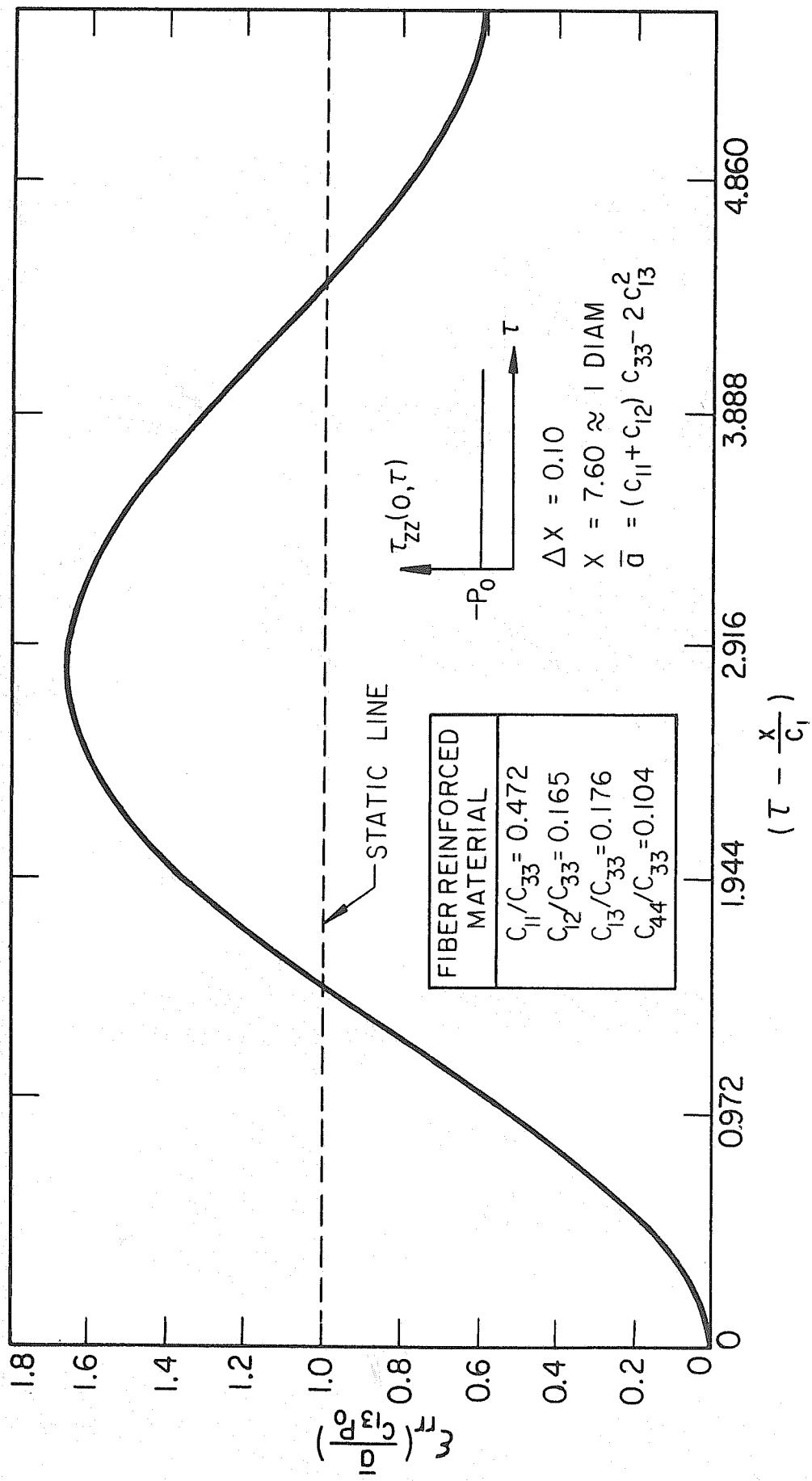


FIG. 2



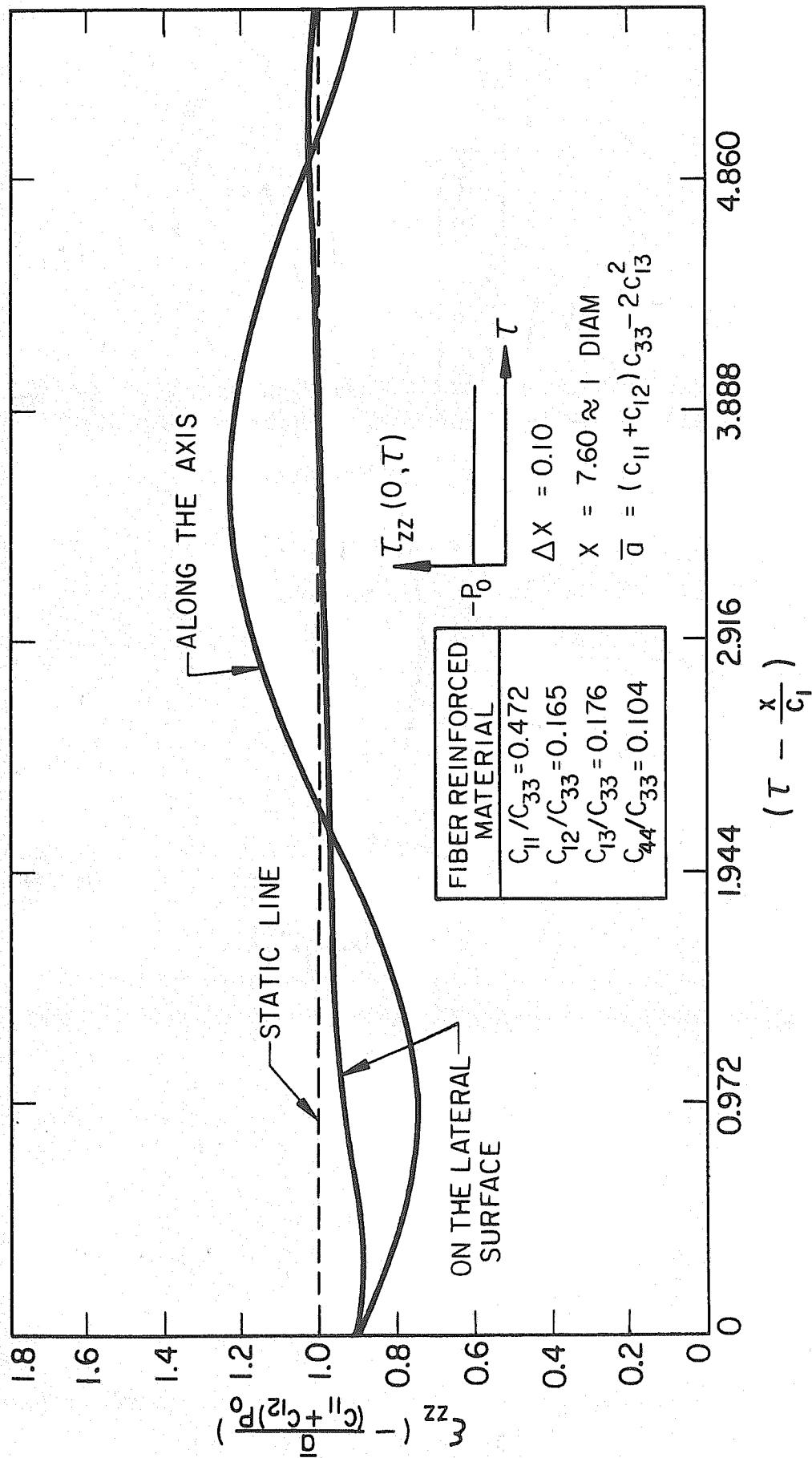
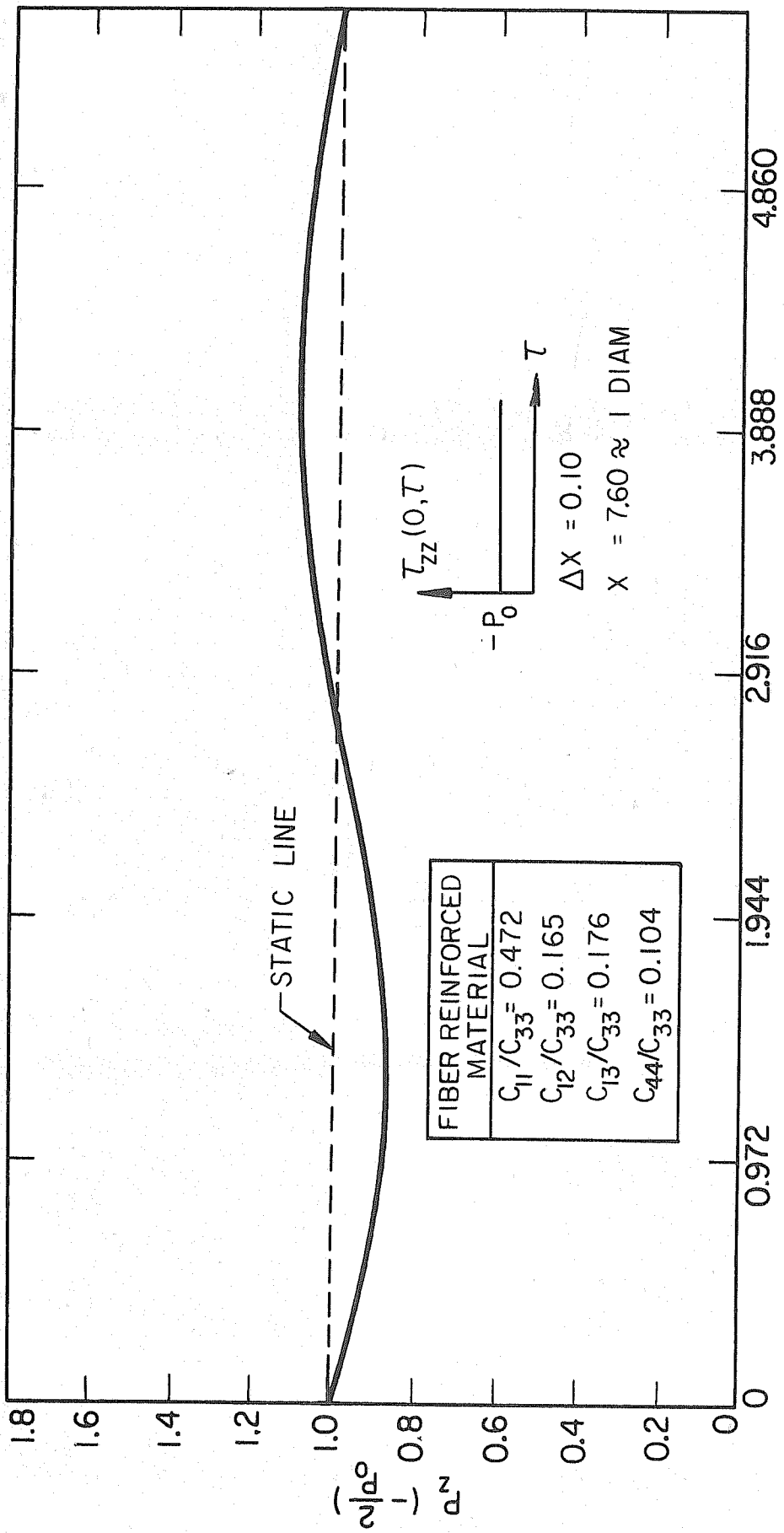
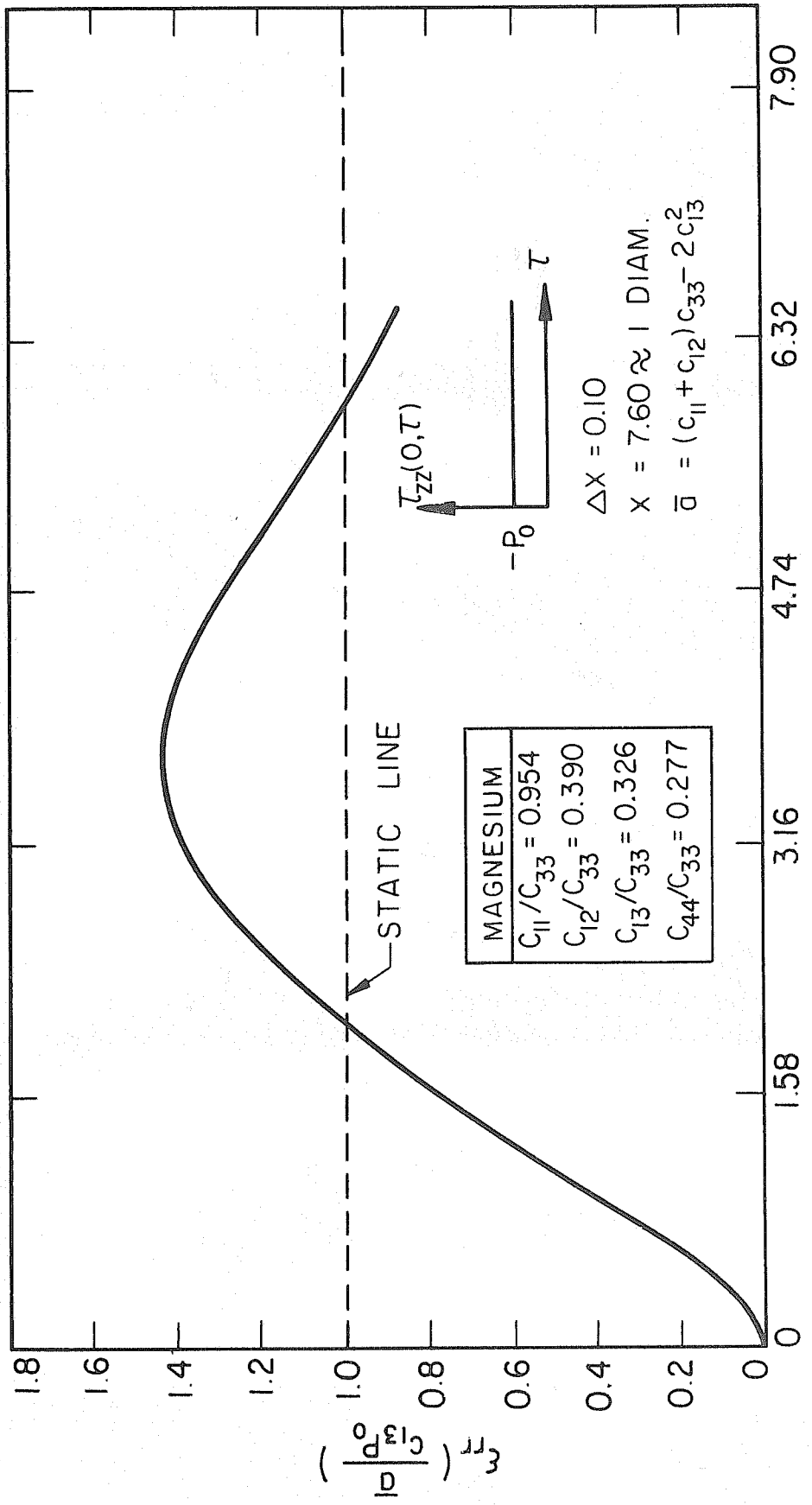


FIG. 3



$$\left( \tau - \frac{x}{c_1} \right)$$

FIG 4



$$\left( \tau - \frac{X}{C_1} \right)$$

FIG. 5

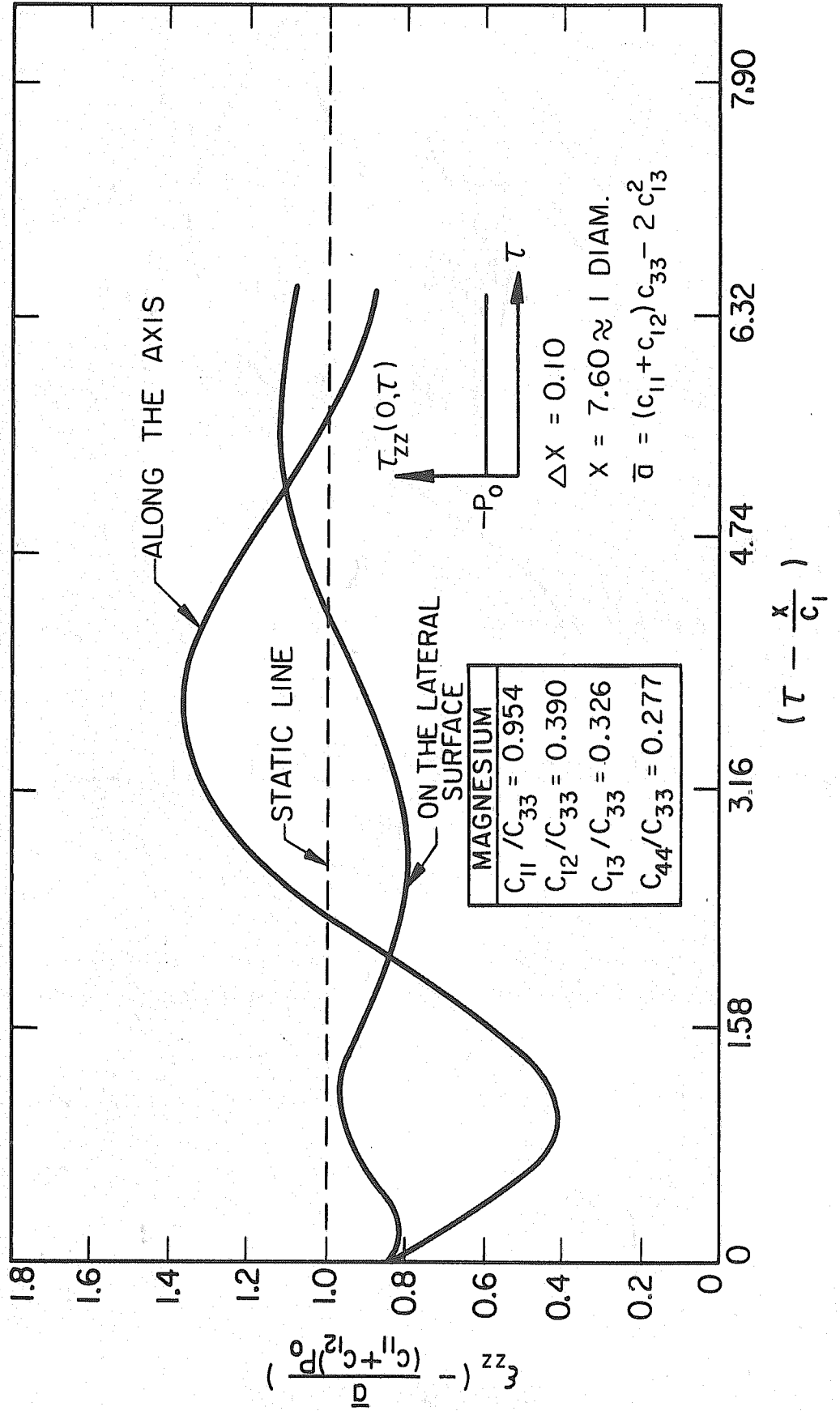


FIG. 6

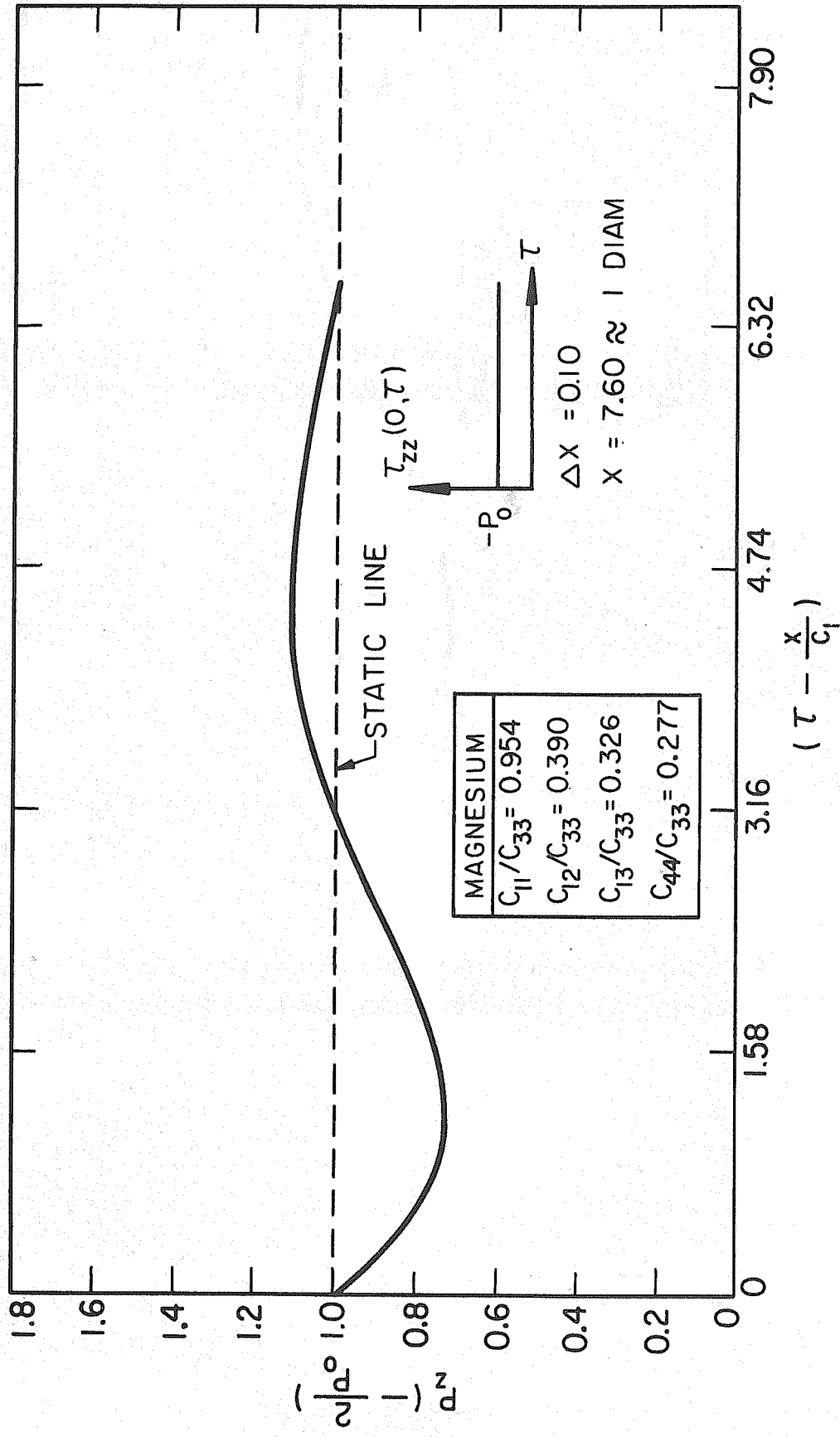


FIG. 7